GEOKINEMATICS OF CENTRAL EUROPE FROM GPS DATA

Alessandro Caporali [1] and Janusz Śledziński [2]

[1] **University of Padova, Department of Geology, Paleontology and Geophysics**

[2] **Warsaw University of Technology, Institute of Geodesy and Geodetic Astronomy**

SUMMARY

In several seismic or potentially seismic areas deformation processes at moderate depth generate deformation at the surface, and the measurement of such surface deformation is an important boundary condition to models of the evolution of interacting blocks before, during and after earthquakes. The network of some 160 permanent GPS stations disseminated in Europe under the European Permanent Network of EUREF and the CERGOP 2 Project of the European Union, with additional local densification stations, provides a valuable contribution to the estimate of the average surface strain rate. The expected strain rate is of the order of 20 – 40 nanostrain per year, corresponding to a velocity change of a few mm/year over distances of some hundreds of km. Consequently, we require accuracies in the velocities of fractions of mm/year, and full control of systematic errors which may mask tectonic signals. Based on our systematic processing of GPS data from permanent European GPS stations covering nearly a decade (1995-2005) we present the large scale velocity flow across most of continental Europe, and the associated horizontal gradient, or strain rate field.

1. INTRODUCTION

The distribution in space and time of geodetically derived strain rate in Central Europe is expected to correlate with the geometry and activity of seismogenic faults, and to provide quantitative information on aseismic geodynamic processes which do imply deformation within an elastic/plastic rather than brittle rheology. Changes of strain rate with time should affect the probability that a fault activates in the short term. The strain rate on an area is only one component in the assessment of a seismic hazard, and other parameters such as the friction coefficient on faults, the dip angle vs. thickness of the brittle layer and, especially, the stress on the rocks left by previous seismic events on the fault, or transferred on the fault from events which took place at nearby faults. By measuring the strain rate, and the regional scale velocity, we therefore address the general deformation affecting a region, such as Central Europe.

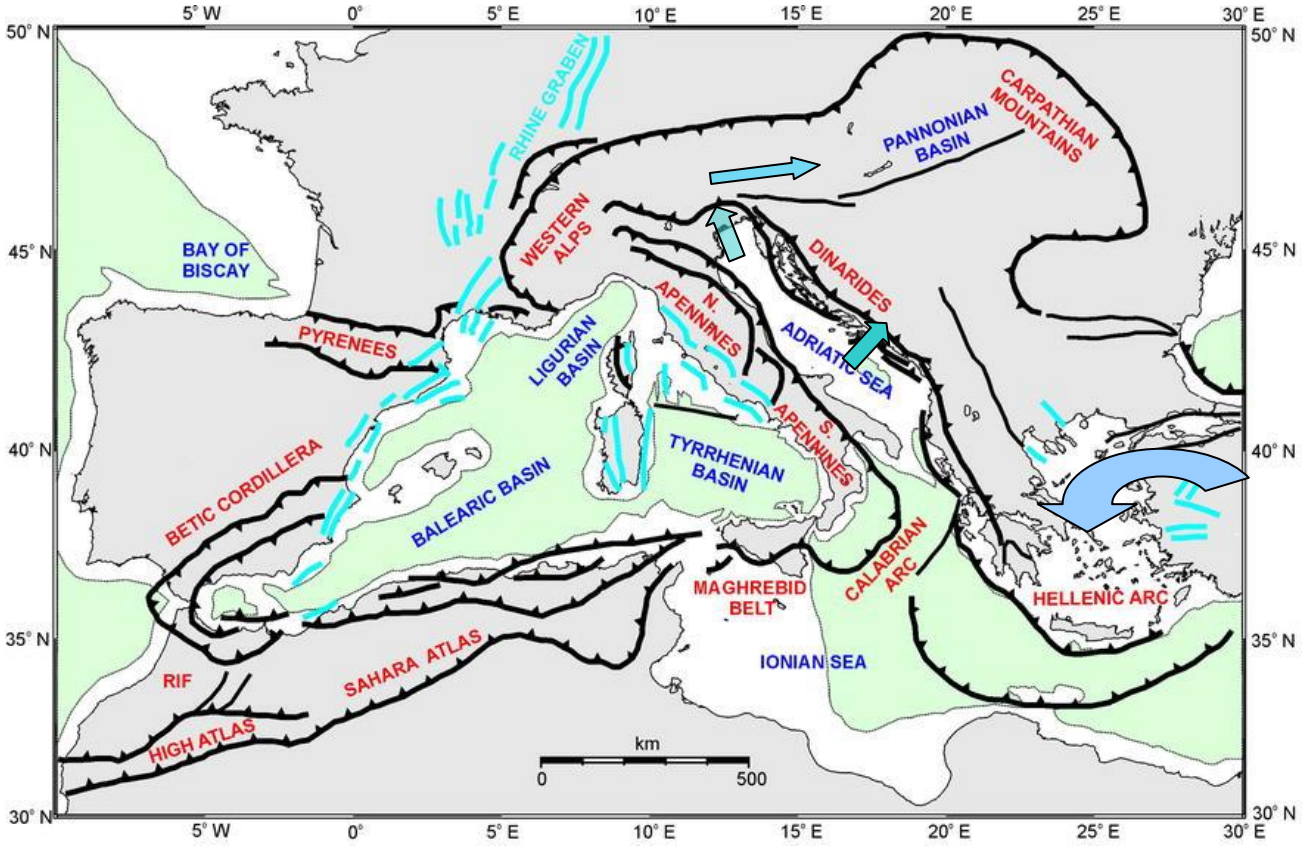

Figure 1. Structural setting of Continental Europe, the Mediterranean and the Hellenic arc, adapted from Jolivet and Faccenna (2000)

The tectonic setting is outlined in Figure 1 (Jolivet and Faccenna, 2000). We expect that the geokinematics of Central Europe is controlled by a) the northwards indentation of Adria into the Eastern Alps, b) the possible lateral escape of the Tauern window eastwards, toward the Pannonian Basin acting as a stress sink (Ratschbacher,et al. 1991a,b; Regenauer Lieb and Petit, 1997); c) active NNE compression along the Dinarides, reflecting the counterclockwise rotation of the Italian peninsula (Mantovani et al., 2000); d) right lateral shear driven by the clockwise rotation of the Anatolian plate, and active convergence along the Hellenic arc. It should be remarked that this is a very crude list: other processes do take place: for example the opening of the Thyrrenian basin, the active convergence and subduction along the Calabrian arc, and the deformation which is associated to the Vrancea Seismic Zone in Romania. We will confine the attention to those large scale processes which can clearly defined by means of geodetic measurements, continuing and extending previous work of Becker et al. (2002), Caporali et al.(2003), Grenerczy et al. (2000,2005), in the framework of the CERGOP Project financed by the European Union (Pesec, 2002).

2. DATA SOURCES

Our analysis is based primarily on weekly SINEX files resulting from network solutions of the EPN, Italian and Austrian networks, and on the SINEX files resulting from the CEGRN campaigns from 1994 to 2003 (Fejes, 2006). These files represent a quantitative picture of a network at an epoch, as they provide coordinates, covariance and constraints.

The weekly SINEX files have been combined into a unique weekly file, thereby realizing A regional densification of the EPN, since the contributing SINEX files are processed

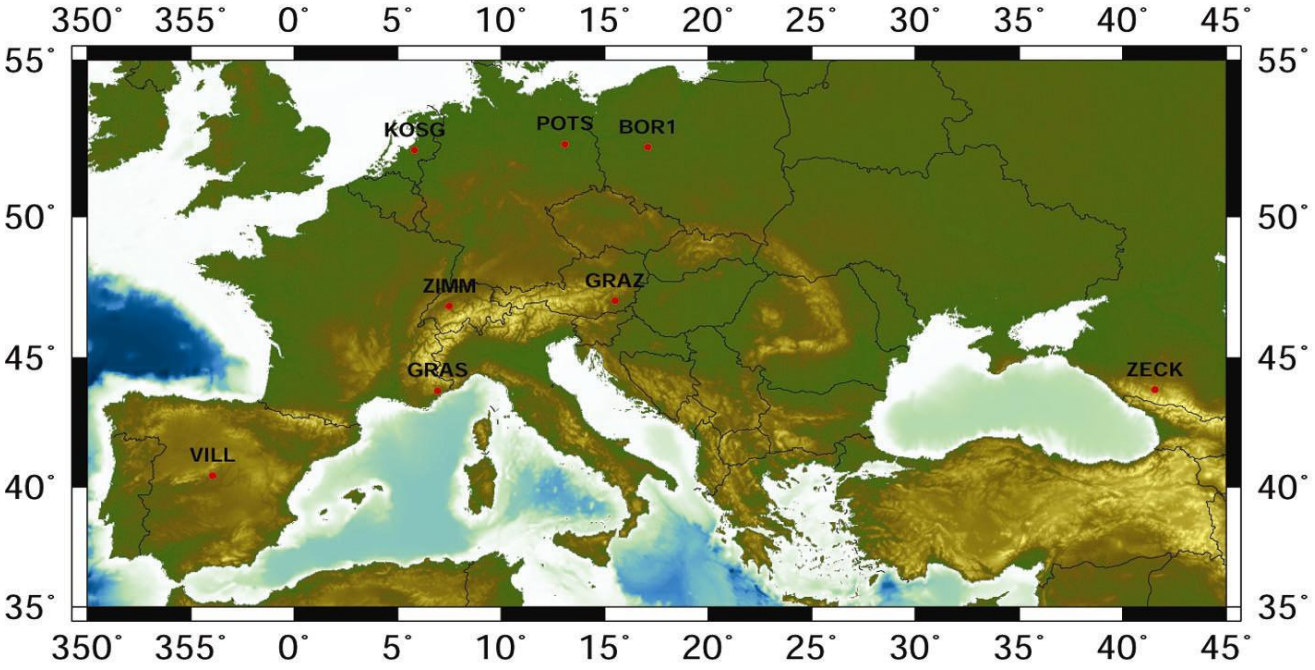

Figure 2. The stations shown were used to define the position and velocity datum, consistently with ITRF2000

exactly in the same manner. Normal equation stacking involving these weekly normal equations plus the campaign CEGRN normal equations, and a unique velocity field is obtained. This multi year solutions is done iteratively, in the sense that one has to ensure that the time series are free of sudden jumps due to occasional events, such as antenna replacement, for example. Velocities are estimated only after correcting the time series for such discontinuities. The constraints which are imposed for realizing a position and velocity datum consistent with ITRF2000 (Altamimi et al. , 2002) are shown in Figure 2 and Table 1.

Table 1. Stations used for the realisation of the ITRF 2000 reference frame

Constraints to IGS/ITRF2000 values

- **BOR1 12205M002 POS**
- **KOSG 13504M003 POS**
- **ZIMM 14001M004 POS VEL**
- **POTS 14106M003 POS VEL**
- **GRAS 10002M006 POS VEL**
- **GRAZ 11001M002 POS**
- **VILL 13406M001 VEL**
- **ZECK 12351M001 VEL**

The datum defining stations have been chosen on the basis of the long term stability of the time series. We refer to Caporali (2003) for a discussion in depth. The statistics of the solve for parameters is summarized in Table 2.
The resulting velocities are shown in Figure 3, for the Central European Area.

Table 2. Statistics of the normal equations stacking done with the Bernese software ADDNEQ to generate the time series and the velocities

STATISTIC OF SOLVED FOR PARAMETERS	#PARAMETERS	#PRE-ELIMINATED
STATION COORDINATES	1116	2706 (BEFORE INV)
STATION VELOCITIES	1053	0
NUMBER OF SOLVE FOR PARAMETERS	2169	2706
TOTAL NUMBER OF PARAMETERS	: 35894517	
TOTAL NUMBER OF OBSERVATIONS	> 53806263	
NUMBER OF SINGLE DIFF. FILES	: 34758	
A POSTERIORI SIGMA OF UNIT WEIGHT	: 0.0034 m	
TOTAL NUMBER OF STATIONS	: 372	

3. STATISTICAL ANALYSIS OF THE VELOCITIES

For further processing of the velocity data we first address the question of the

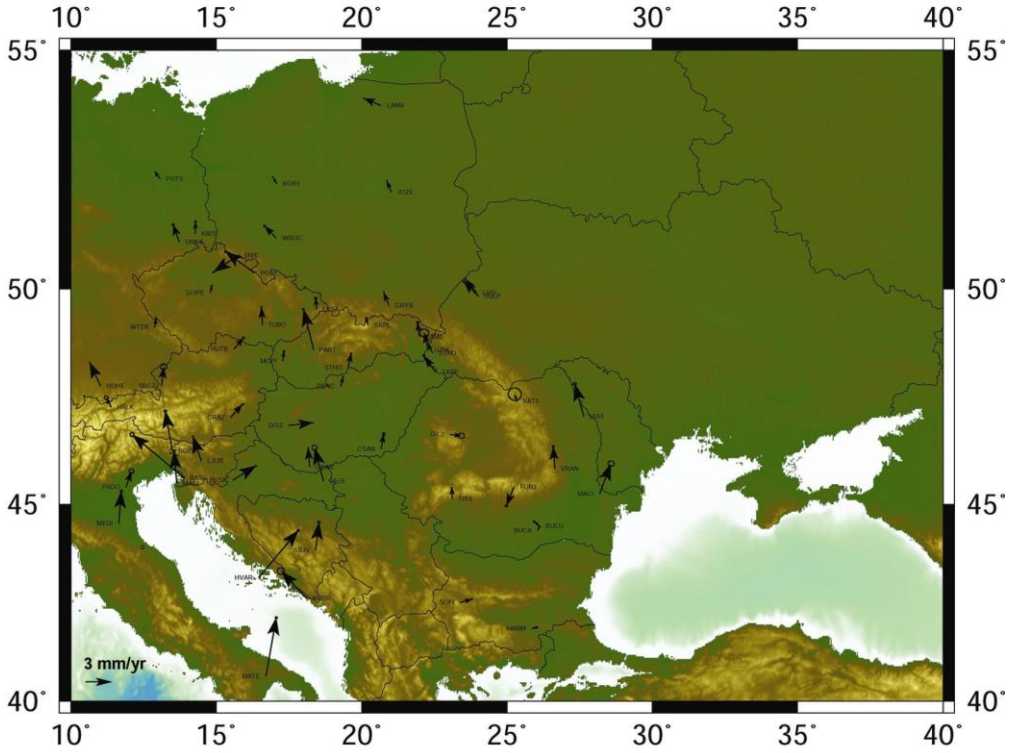

Figure 3. The velocities in the Central European area resulting from the time series analysis, after subtraction of the NUVEL1A NNR predictions. Of particular interest is the northwards convergence of Adria into the Eastern Alps (negative velocity gradient moving north), which is flanked by an eastward motion toward the Pannonian/Carpathian area

decorrelation length of the horizontal velocity set. We intend to compute velocity gradients by least squares collocation. For this purpose a covariance function is needed in order to represent the fall off of the correlation coefficient with the lag distance. In Figure 4 we represent the covariance of the horizontal components of the velocities, and the best fitting function of the type given in Equation 1.

Once the covariance function has been assigned a characteristic distance d_0 consistent with the statistical property of the data, then the velocity and the associated uncertainties can be computed at any point according to Equation 2.

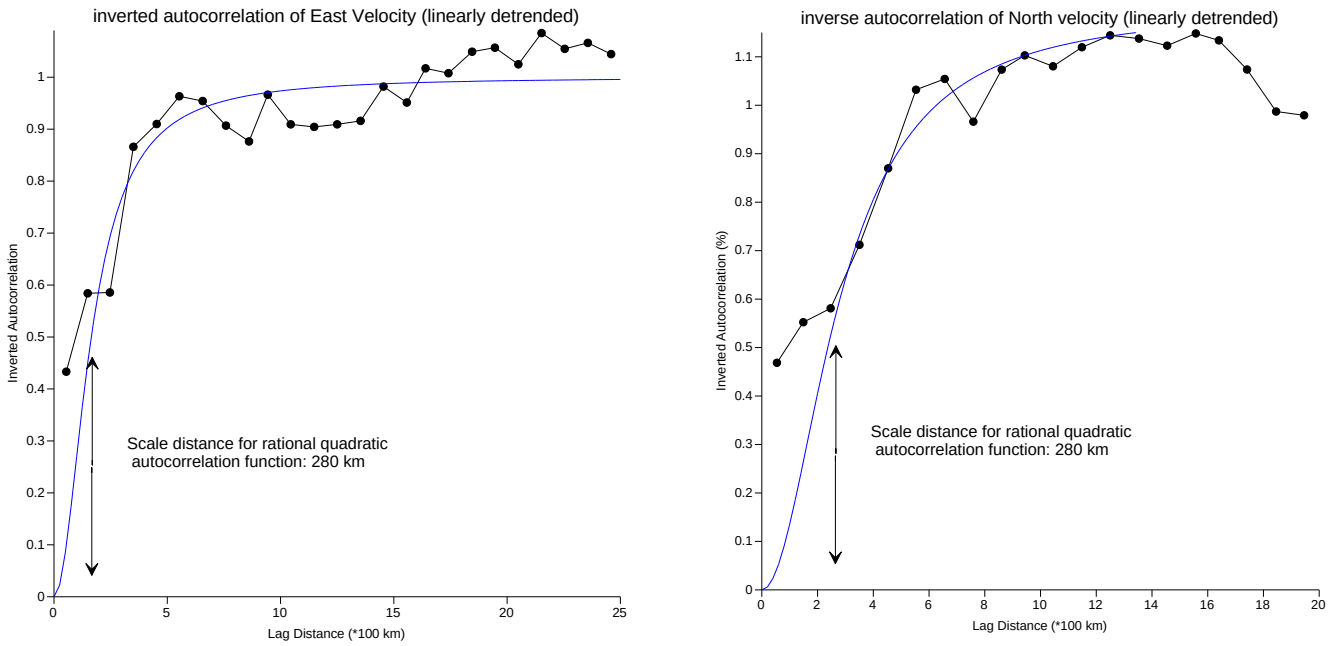

Figure 4. Correlation of the east and north velocity as a function of the lag distance, and the best fitting curve given by eq. 1 and d_0=280 km.

$$C_{ij}(d) = \frac{C_{ij}(0)}{1+\left(d/d_0\right)^2} \quad i,j = e(ast), n(orth); \quad C(d) = \begin{bmatrix} C_{nn} & C_{en} \\ C_{en} & C_{ee} \end{bmatrix}$$

$$\begin{bmatrix} v_n \\ v_e \end{bmatrix}_{grid-node} = \sum_s C(d_{grid-node,s}) \sum_{s'} C^{-1}(d_{s,s'}) \begin{bmatrix} v_n \\ v_e \end{bmatrix}_{s'} \quad s,s' = station \quad indeces \qquad \textbf{(2)}$$

$$\begin{bmatrix} \sigma_{nn} \\ \sigma_{ee} \end{bmatrix}_{grid-node} = \left\{ \left[\sum_s C(d_{grid-node,s}) \sum_{s'} C^{-1}(d_{s,s'}) \right]^T E^{-1}{}_{s's'} \left[\sum_s C(d_{grid-node,s}) \sum_{s'} C^{-1}(d_{s,s'}) \right] \right\}^{-1}$$

In the propagation of the variance (the second of eq. 2) the Matrix E is the matrix of the variances of the individual velocities at the station points. Because the formal uncertainties estimated by the least squares adjustment program are in most cases too optimistic, they can be replaced by the Allan variances, if the series is long and dense enough to enable a meaningful computation, or by the formal variances rescaled by a factor of 4 (Caporali, 2003).

The estimated value of the decorrelation length d_0=280 km has a mechanical interpretation.

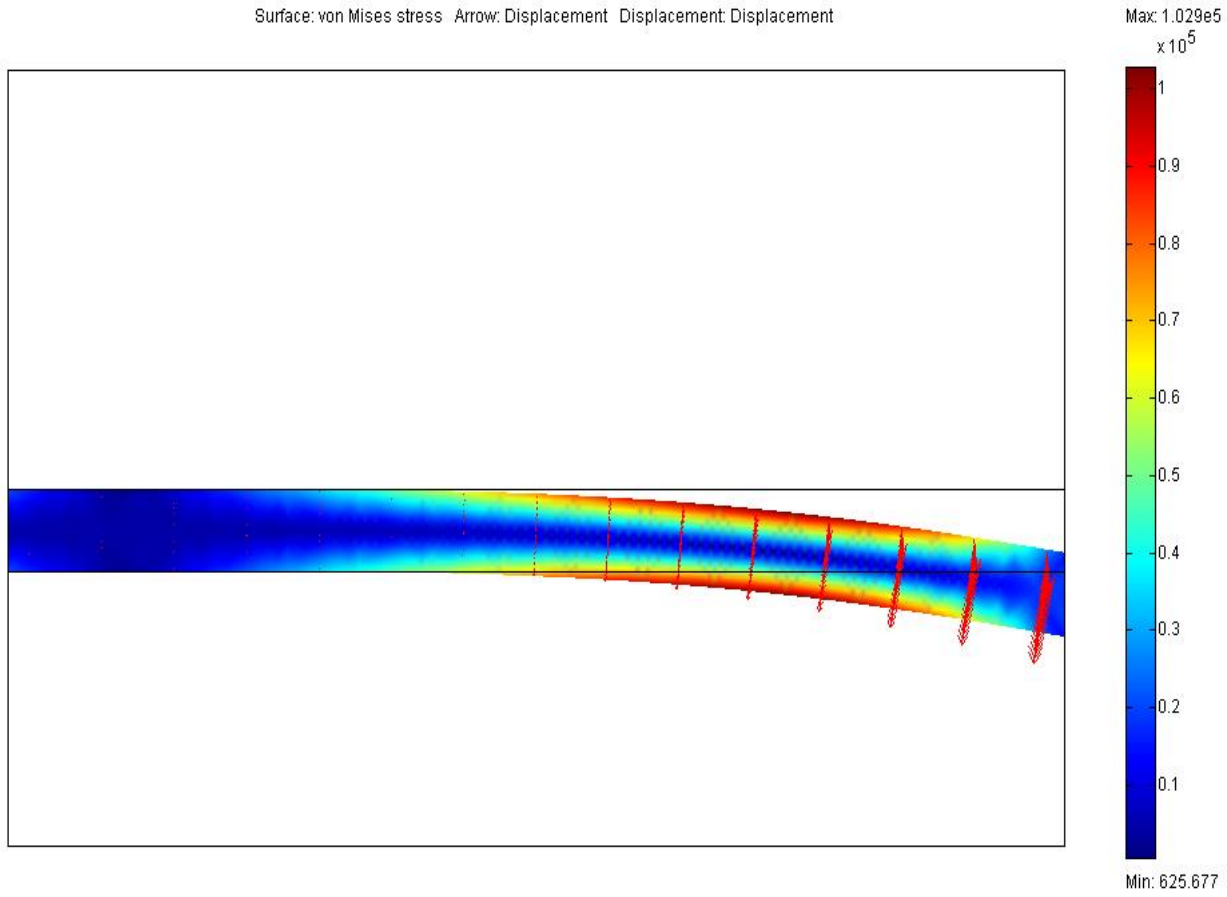

Figure 5. Bending of a semi infinite elastic plate, isostatically supported and subject to a vertical load and / or a torque at the free end. The wavelength of the resulting deformation can be computed analytically with eq.5

Consider a semi infinite elastic plate supported isostatically and bending under the action of an applied load or momentum at the free end. The governing equation resulting from the balance conditions is

$$D\frac{d^4w}{dx^4}+(\rho_m-\rho_c)gw=0 \qquad (3)$$

Where we have introduced the coefficient of flexure:

$$D = \frac{Eh^3}{12(1-\nu^2)} \qquad (4)$$

We have denoted by E the young modulus, ν the Poisson ration and h the thickness of the plate, g is the gravity constant and ρ_m-ρ_c is the mantle/crust density contrast providing the isostatic buoyancy.

The analytical solution is given, in the case of a vertical load at the free end, by

$$w(x) = w_0 e^{-\frac{x}{\alpha}} \cos\frac{2\pi x}{\alpha} \qquad (5)$$

Where we have introduced the flexural parameter

$$\alpha = \left[\frac{4D}{(\rho_m - \rho_c)g}\right]^{1/4} \qquad (6)$$

If E=70 Gpa, ν=0.25, density contrast 600 kg/m^3 and plate thickness ~ 27 km, then the flexural parameter α ~ 280 km. This means that the decorrelation length we have determined statistically corresponds to the wavelength at which an elastic crust deforms under the action of a load, taking into account isostasy.

4. ESTIMATING STRAIN RATES

For deformation analyses it is crucial to know how velocity changes spatially. The horizontal velocity gradient can be computed by differentiating eq.2:

$$\begin{bmatrix} v_{n,n} & v_{n,e} \\ v_{e,n} & v_{e,e} \end{bmatrix}_P = \sum_s \begin{bmatrix} \frac{\partial C}{\partial n} & \frac{\partial C}{\partial e} \\ \frac{\partial C}{\partial n} & \frac{\partial C}{\partial e} \end{bmatrix}_{P,s} \sum_{s'} \left[C(d_{s,s'}) + W_{ss'}\right]^{-1} \cdot \begin{bmatrix} v_n \\ v_e \end{bmatrix}_{s'} \qquad s, s' = station \quad indeces \qquad (7)$$

This matrix can be split into a symmetric and a anti symmetric part. The symmetric part represents strain rate, whereas the anti symmetric part represents a rigid rotation

and is, hence, ignorable for our purposes. The symmetric part can eventually be diagonalized, yielding the familiar eigenvectors or principal directions of strain rate:

$$\varepsilon_1 = \frac{v_{n,n} + v_{e,e}}{2} + \sqrt{\left(\frac{v_{e,e} - v_{n,n}}{2}\right)^2 + \left(\frac{v_{e,n} + v_{n,e}}{2}\right)^2}$$

$$\varepsilon_2 = \frac{v_{n,n} + v_{e,e}}{2} - \sqrt{\left(\frac{v_{e,e} - v_{n,n}}{2}\right)^2 + \left(\frac{v_{e,n} + v_{n,e}}{2}\right)^2} \qquad \textbf{(8)}$$

$$\sin 2\theta = \frac{v_{e,n} + v_{n,e}}{\varepsilon_2 - \varepsilon_1}; \cos 2\theta = \frac{v_{e,e} - v_{n,n}}{\varepsilon_1 - \varepsilon_2}$$

The uncertainty in the components of the strain rate tensor are obtained by collocation starting from the formal uncertainties of the velocities at the stations:

$$\begin{bmatrix} dv_{n,n} & dv_{n,e} \\ dv_{e,n} & dv_{e,e} \end{bmatrix}_P = \sum_s \begin{bmatrix} \frac{\partial C}{\partial n} & \frac{\partial C}{\partial e} \\ \frac{\partial C}{\partial n} & \frac{\partial C}{\partial e} \end{bmatrix}_{P,s} \sum_{s'} \left[C(d_{s,s'}) + W_{ss'}\right]^{-1} \cdot \begin{bmatrix} \sigma_n \\ \sigma_e \end{bmatrix}_{s'} \quad s, s' = station \quad indeces \qquad \textbf{(9)}$$

Differentiating eq. 8 and using eq. 9 for the uncertainties in the velocity gradients we finally obtain the formal uncertainties in the eigenvalues and in the azimuth angle:

$$d\varepsilon_{1,2} = \frac{dv_{n,n} + dv_{e,e}}{2} \pm \frac{\frac{\left(v_{e,e} - v_{n,n}\right)\left(dv_{e,e} - dv_{n,n}\right)}{2} + 2\varepsilon_{e,n} d\varepsilon_{e,n}}{2\sqrt{\left(\frac{v_{e,e} - v_{n,n}}{2}\right)^2 + \left(\varepsilon_{e,n}\right)^2}} \qquad \textbf{(10)}$$

$$d\theta = \cos^2 2\theta \left[\frac{d\varepsilon_{e,n}}{v_{e,e} - v_{n,n}}\right] - \frac{\varepsilon_{e,n}\left(dv_{e,e} - dv_{n,n}\right)}{\left(v_{e,e} - v_{n,n}\right)^2}$$

To represent the uncertainty in the strain rate tensor we use the symbol in Figure 6. The coloured part is two times the uncertainty of the eigenvector, and the opening of the cone is plus/minus the uncertainty in the angle. In principle we have different uncertainties for the two eigenvectors. To avoid confusion we choose to plot the largest uncertainty for one component only.

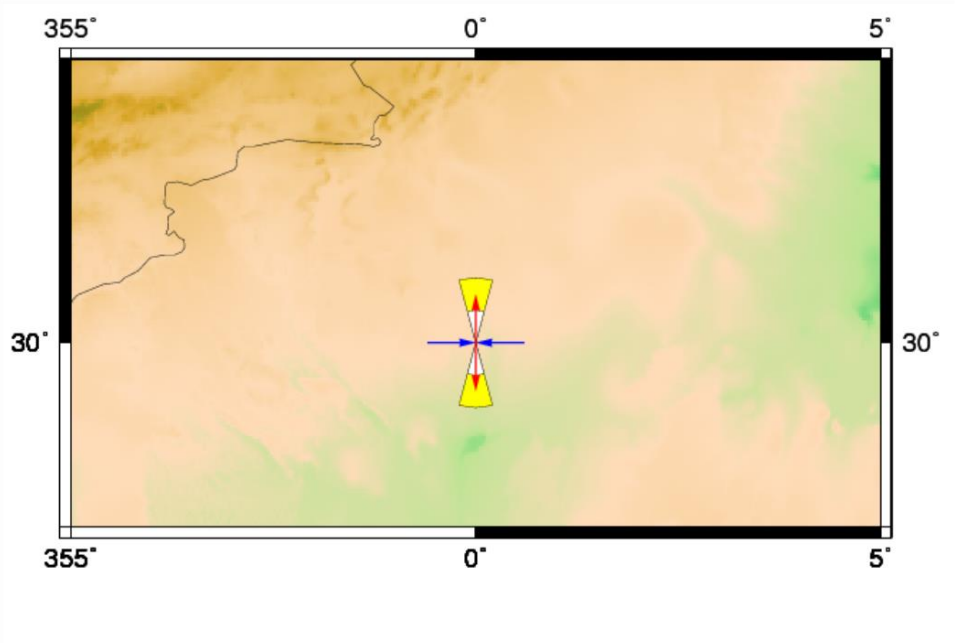

Figure 6. The uncertainty in the strain rate eigenvectors is represented by a cone of amplitude equal to +/- the uncertainty in the angle and an uncertainty range equal to +/- the maximum uncertainty of the eigenvalues computed with eq. 10

A final question is where to compute the strain rates. There exist two schools of thought. One school computes the strain rate on a regular grid, and propagating the uncertainty to account for the loss of accuracy as one moves away from the data points. The other school is more conservative, in the sense that the strain rates are computed only at those points where the estimates are sufficiently well constrained. Hence the strain rate map is patchy, but most reliable. We adhere to this last approach. To ensure maximum accuracy and consistency with the statistical properties of the velocity set we compute the strain rates at the location of those stations which are surrounded, by four or more stations with known velocity within a radius equal to the decorrelation distance d_0, as shown in Figure 7.

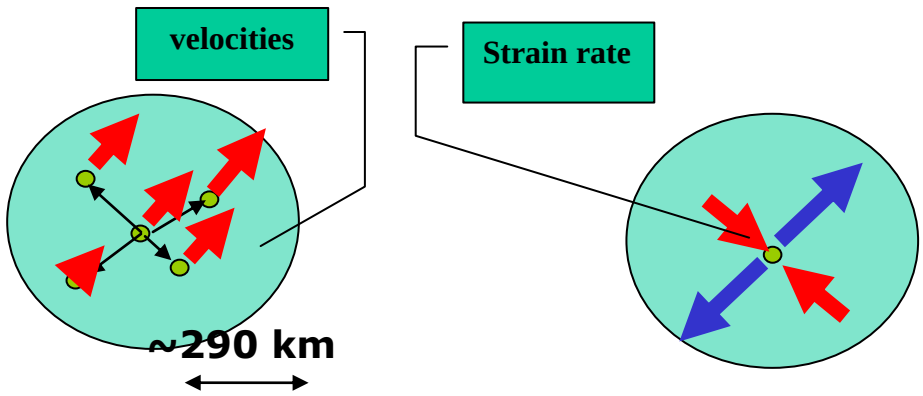

Figure 7. Strain rate is computer at a central location of measured velocità surrounded by data points in the four quadrants, within the decorrelation distance

5. THE STRAIN RATE IN CENTRAL EUROPE FROM THE CERGOP DATA SET

We report in Figure 8 the strain rate map we have computed with the CERGOP data set, according to the procedure outlined in the previous sections.

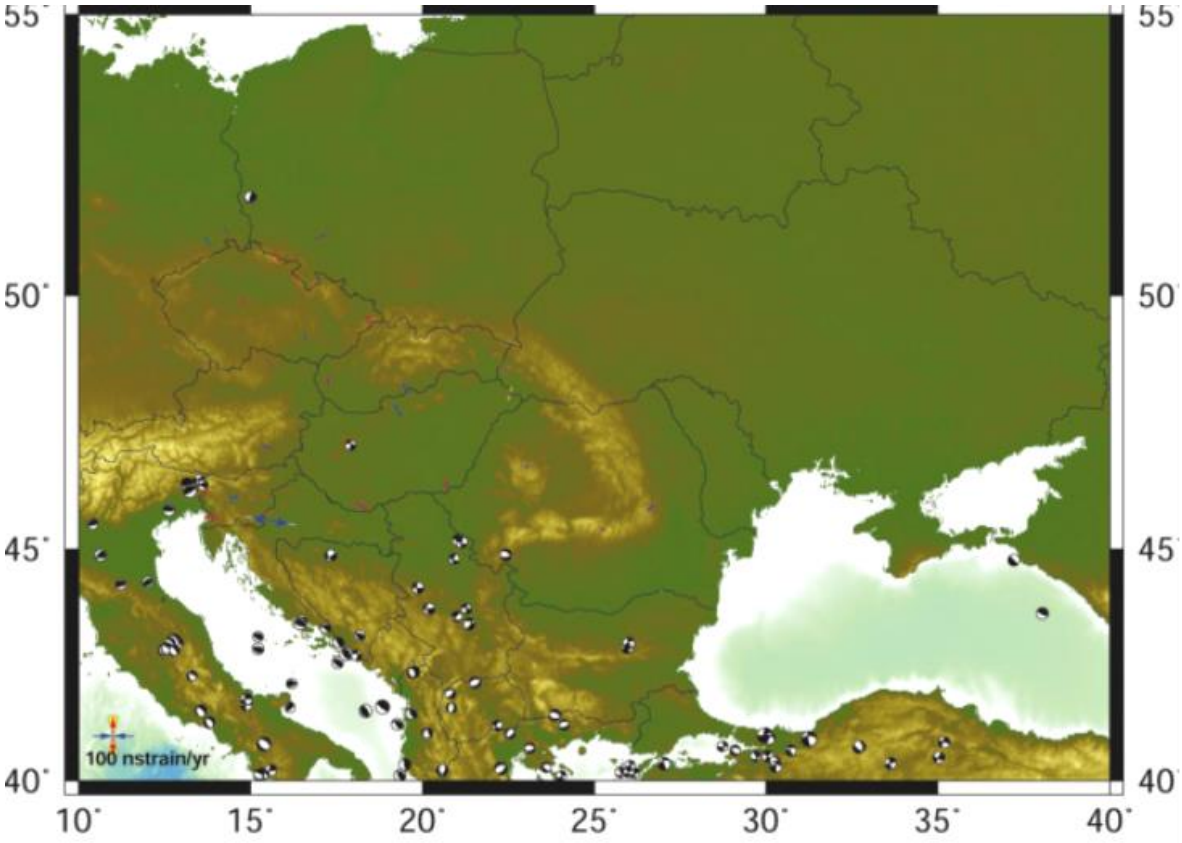

Figure 8. The strain rate computed with the CERGOP velocità set at sufficiently constrained data points. Overall the deformation appears very small, except in Slovenia and Styria where the extensionl regime probably reflects the deformation in the Pannonian basin. CMT's of M>5 are from the Harvard catalogue (http://www.seismology.harvard.edu/projects/CMT/)

Our conservative approach enables us to compute strain rates only at few points in the Pannonian basin, Carpathians and Tatra mountains. Overall the strain rates are small, except in Slovenia (Vodopivec et al., 2005) where they are close to 100 nstrain/year, extensional . This behavior probably reflects the extensional processes in the Pannonian basin, somewhat more north. Small (of the order of 10 nstrain/year) are reported in the Carpathians and Tatra mountains, confirming that these regions are essentially stable. On the other hand, seismicity is concentrated in Macedonia, Dinarids and Greece, whereas the seismic events in Vrancea are probably too deep to leave a deformation signature at the surface (Rus et al., 2005).

6. CONCLUSION

The velocities of GPS stations we have estimated for Central Europe, as they result from the CERGOP project, reflect a moderate deformation regime, as confirmed by the relatively low surface seismicity, compared to neighbouring Greece or Dinarids/Eastern

Alps. However it would be unwise to conclude that low strain rates imply low seismic risk. There are many examples in which the pre seismic phase coincides with a low strain rate, because the rocks stop deforming linearly, while stress continues to be applied.

In this sense the role of the continuing effort by Central European countries to monitor the position of GPS stations should be emphasized. The increasing densification of velocity points will enable the strain rates to be computed reliably at additional locations, making more clear the deformation picture which begins to emerge already now.

ACKNOWLEDGEMENT

This work is done in the framework of the EU Project CERGOP 2, led by P. Pesec, within the 5. Framework Programme.

REFERENCES

Altamimi, Z., Sillard, P., C. Boucher, 2002. ITRF2000: a new release of the International Terrestrial Reference Frame for earth science applications. *J. Geophys. Res. 107(B10), 2214, doi: 10.1029/2001JB000561.*

Becker, M., Cristea, E., Figurski, M. et al., 2002, Central European Intraplate Velocities from CEGRN Campaigns, *Reports on Geodesy 1(61):83.*

Caporali,, A., 2003, Average strain rate in the Italian crust inferred from a permanent GPS network. Part 1: Statistical Analysis of Time Series of Permanent GPS Stations, *Geophys. J. Int.155, 241-253.*

Caporali,, A., Martin, S. ,Massironi, M., 2003, Average strain rate in the Italian crust inferred from a permanent GPS network. Part 2: Strain rate vs. seismicity and structural geology, *Geophys. J. Int.155, 254-268.*

Fejes, I., 2006, Consortium for Central European GPS Geodynamic Reference Frame (CEGRN Consortium), in N. Pinter et al. (eds.) The Adria Microplate: GPS geodesy, Tectonics and Hazards, Springer Verlag, The Netherlands, 183-193.

Grenerczy, G., A. Kenyeres, I. Fejes, 2000, Present crustal movement and strain distribution in Central Europe inferred from GPS measurements, *J. Geophys. Res., 105(B9), 21835-21846, 10.1029/2000JB900127.*

Grenerczy G., G. Sella, S. Stein, A. Kenyeres , 2005, Tectonic implications of the GPS velocity field in the northern Adriatic region, *Geophys. Res. Lett., 32, L16311, doi:10.1029/2005GL022947.*

Jolivet, L., and Faccenna, C., 2000, Mediterranean extension and the Africa-Eurasia collision: *Tectonics, 19, 1095–1106.*

Hefty, J., 2005, GPS data analysis and the definition of reference frames, *Reports on Geodesy 4(75), 47-52.*

Mantovani, E., M. Viti, D. Albarello, C. Tamburelli, D. Babbucci and N. Cenni, Role of kinematically induced horizontal forces in Mediterranean tectonics: insight from numerical modeling, *J. Geodyn. 30, 287-320, 2000.*

Pesec, P., 2002, CERGOP 2,a multipurpose and multidisciplinary sensor array for environmental research in Central Europe, Geophys. Res. Abs. Vol.4., EGS General Assembly.

Ratschbacher, L., O. Merle, P. Davy and P. Cobbold, Lateral Extrusion in the Eastern Alps, Part 1: Boundary conditions and experiments scaled for gravity, *Tectonics, 10, 245-256, 1991.*

Ratschbacher, L., W. Frisch, H.G. Linzer, and O. Merle, Lateral Extrusion in the Eastern Alps, Part 2: Structural analysis, *Tectonics, 10, 257-271, 1991.*

Regenauer-Lieb,K. and J.P. Petit, Cutting of the European continental lithosphere; plasticity theory applied to the present Alpine collision, *J. of Geophys. Res., 102, 7731-7746, 199*7.

Rus, T., Buse, I., Besutiu, L., Stanescu, G., Stoian, I., and Nacu, V., 2005, Status of the activities performed within the CERGOP 2 project in Romania, *Reports on Geodesy 4(75), 155-172.*

Vodopivec, F., Placer, L., Poljak M., and Kogoj, D. ,2005, Geodynamics of North Mediterranean and Eastern Alps, *Reports on Geodesy 4(75), 151-153.*